Journal of Guidance, Control, and Dynamics, Available online 7 November 2023
DOI:10.2514/1.G007169

# Approximation of Achievable Robustness Limit Based on Sensitivity Inversion

Namhoon Cho * and Hae-In Lee †
*Cranfield University, Cranfield, Bedfordshire, MK43 0AL, United Kingdom*

## I. Introduction

The sensitivity function defined as the closed-loop transfer function from the exogenous input to the tracking error is central in the multi-objective design and analysis of a feedback control system. Its frequency response determines many performance characteristics of the closed-loop system such as disturbance attenuation, reference tracking, and robustness against uncertainties and noise. It is well-known that the nominal sensitivity peak, i.e., the $\mathcal{H}_\infty$-norm of sensitivity function, is a direct measure of stability robustness, because the sensitivity magnitude quantifies both the attenuation of the effect of external disturbances on the closed-loop output and the variations of the closed-loop system with respect to the plant perturbations.

Minimisation of the sensitivity peak is naturally a design direction for maximal robustness, however, the trade-off between conflicting design goals and the structural constraints fundamentally limit the achievable sensitivity improvement in a feedback control system. Among others, the conservation of the logarithm of sensitivity magnitude integrated over all frequencies known as the Bode integral constraint indicates that improvement in a frequency band comes at the inherent cost of degradation in another frequency region. Moreover, the physical hardware on which a control system operates places additional bandwidth limitations, in turn, the sensitivity penalty in the high-frequency region cannot be arbitrarily minimised. In this respect, frequency-dependent shaping of the sensitivity magnitude is an important concern in addition to peak minimisation.

Identification of the fundamental limitations in the achievable sensitivity characteristics should preferably precede controller design. It is impossible to achieve an arbitrarily specified set of performance goals through feedback due to the presence of the fundamental constraints [1]. The boundaries of achievable performance characteristics are determined by the physical properties of the plant rather than the detailed specifics of the controller as it was discussed well in [2] with the fundamental feedback control limitations posed by the Bode sensitivity integral constraint in statically unstable X-29 forward-swept-wing aircraft as an example for illustration. This implies that the design requirements belonging to the infeasible region can never be achieved by means of changing the intrinsic attributes of a controller such as its order, loop structure, gains, etc. The choice of the control design method is also irrelevant to the solution space boundaries.

*Research Fellow, Centre for Autonomous and Cyber-Physical Systems, School of Aerospace, Transport and Manufacturing, n.cho@cranfield.ac.uk, AIAA Member
†Lecturer in Autonomous Systems, Centre for Autonomous and Cyber-Physical Systems, School of Aerospace, Transport and Manufacturing, haein.lee@cranfield.ac.uk

Therefore, it is highly desirable to specify realistic design requirements based on the identified limit of attainable performance in terms of the sensitivity function so as to prevent unnecessary expenses in time and computational resources dealing with impossible goals. It was clearly demonstrated in the X-29 case study of [2] that one can determine the possibility of finding an acceptable controller with given stability margin criteria simply through the Bode sensitivity integral calculation considering only the rough knowledge of plant unstable pole and bandwidth characteristics. The remarkable similarity between the frequency response of the actual final flight controller and the simple prototype derived based on the fundamental sensitivity constraint when the situation is marginal was also evidenced in [2].

Earlier studies on multivariable robust control have completely characterised the theories and developed respective methods for sensitivity optimisation, but their intricacy over the classical control has posed an unnecessary difficulty in using the optimisation methods for identification of the achievable performance limit with consistent physical understandings about the plant characteristics. The studies on $\mathcal{H}_\infty$-optimal control established conventional methodologies for sensitivity minimisation [3–6]. The set of all possible proper stabilising controllers for the given plant is first described with the Youla-Kucera parametrisation. Desensitisation is then performed by minimising the $\mathcal{H}_\infty$-norm of weighted sensitivity within the stabilising parametrisation. This approach suffers from the lack of a general rule for determining an appropriate structure and parameters of the weighting functions for shaping. Another difficulty may arise due to unnecessarily high order of the resultant controller. Nevanlinna-Pick interpolation theory is another branch of methods developed for more direct shaping of sensitivity magnitude without resorting to the frequency weighting function [7–9]. Analytic interpolation facilitates direct shaping of sensitivity magnitude profile while guaranteeing the constraints for internal stability and controller degree, however, this method has gained relatively a limited attention of practitioners. More recently, the fixed-structure $\mathcal{H}_\infty$ method based on non-smooth optimisation technique has been developed and employed for multi-objective tuning with the loop structure specified a priori [10–14]. Although the existing methods now provide a wealth of optimisation techniques for sensitivity shaping, the optimisation-based methods are not widely used for the purpose of identifying the achievable performance limit because the insights from classical control still dominate design practices and many practitioners find the optimisation techniques difficult to use.

The fundamental limitations and performance/robustness bounds have been studied extensively since the control engineer can approach a particular design problem while being aware of what can be achieved as the result of design [1, 15, 16]. A wide range of works done in this area are focused on Single-Input-Single-Ouput (SISO) systems [17–24] including both discrete-time [22–24] and continuous-time [18–21] formulations. The notion of achievable robustness has been characterised for various forms of uncertainties such as real plant coefficient uncertainty [22, 23], $\mathcal{H}_\infty$-norm bounded numerator uncertainty, normalised coprime factor uncertainty [20], a class of multiplicative uncertainties [17], and etc. The achievable robustness analysis for the SISO case is important in that the majority of practical applications depend on SISO control and it is more amenable to clear development of underlying theory than the multivariable case. For missiles, most lateral autopilots with acceleration and angular rate feedback are designed with SISO architecture,

despite the controllers can be composed of various structures [25]. The situation is similar in aircraft control like the one discussed in [2]. Therefore, a tool for estimation of achievable maximal robustness subject to plant characteristics in SISO case is particularly important for flight vehicle system development.

The primary objective of this work is to devise a practical procedure for reasonably low-order approximation of the best achievable robustness based on inversion of a desired sensitivity profile that complies with the fundamental limitations of feedback control in order to be realisable. The focus is on the development of a process that does not rely on numerical optimisation but involves only a small number of bandwidth-related parameters to easily handle the design trade-off. To this end, this study develops the simplified analysis shown in [2, 26] into a systematic method. For the sake of clarity in explaining the main ideas, the present study first considers Linear Time-Invariant (LTI) SISO plants that can either be open-loop stable or unstable but have no zero in the closed right-half plane (RHP). The proposed method proceeds in several steps. The constraints that a sensitivity function of an internally stable closed-loop system should satisfy are identified first. The ideal sensitivity magnitude prototype regarding the Bode integral constraint and the bandwidth limitation is then proposed. Next, the desired sensitivity function is constructed in an elementwise manner so that its magnitude closely resembles the ideal prototype while guaranteeing it to be of a realisable structure as well. In this way, an open-loop frequency response can finally be obtained by inversion of the constructed sensitivity function without incurring unstable pole-zero cancellation between the plant and the controller. In a similar line of reasoning, this study discusses the case of nonminimum-phase plants as well where the presence of RHP zero prohibits direct inversion of the desired sensitivity function for obtaining the open-loop transfer function. Instead, the proposed method solves a relaxed form of weighted sensitivity optimisation problem by considering the inverse of the desired sensitivity function encoding resemblance to the ideal magnitude prototype as the frequency-dependent weighting function.

The proposed approximation method enables rough yet rapid identification of the best achievable robustness characteristics for a given plant with physical understandings about the desired low-frequency performance. A main practical value of the proposed sensitivity inversion method is that it yields an approximation of the optimal robustness achievable by the given physical hardware without exhaustive parametric search or computationally-demanding optimisation. Thus, the simplified method is useful for i) methodical study of the achievable frequency domain performance in the early stages of plant configuration development and also for ii) setting up the design requirements for subsequent detailed design of a controller. More specific to the aerospace control applications, the exact inversion of desired sensitivity is appropriate for the analysis of inner-loop angular rate tracking controller since the longitudinal short-period mode dynamics usually does not place a zero in the RHP at the angular rate channel. Also, the approximate inversion of desired sensitivity suits well with the analysis of normal acceleration tracking controller where the associated plant usually has a zero in the RHP. The feasibility of certain autopilot performance requirements can be verified by using the estimates of the maximum stability margins. Numerical simulation using a statically unstable agile missile model showed that the approximate open-loop frequency response is similar to the results obtained by mixed-sensitivity

$\mathcal{H}_\infty$-optimisation around the frequency associated with control.

This Note is organised as follows: Section II introduces the preliminaries. Section III presents the simplified sensitivity inversion method for approximation of the best achievable robustness. In Sec. IV, illustrative analysis examples considering pitch rate and normal acceleration tracking control for a statically unstable missile validate the practicality of the proposed method. Section V summarises the concluding remarks.

## II. Preliminaries

This section briefly describes the basic definitions and properties of a feedback control system in relation to the sensitivity function as the preliminaries.

### A. Sensitivity Function

In this Note, we consider the one-degree-of-freedom, i.e., one input port, controller connected to the plant with the unity negative feedback structure as shown in Fig. 1. In Fig. 1, the systems $C(s)$ and $P(s)$ represent the controller and the plant dynamics, respectively. The bounded scalar signals $r(t)$, $y(t)$, $u(t)$ denote the exogenous reference, the output, and the input, respectively, and $e(t) = r(t) - y(t)$ is the tracking error. The plant $P(s)$ is considered to be a SISO, LTI, deterministic system for which transfer function representation is proper and rational.

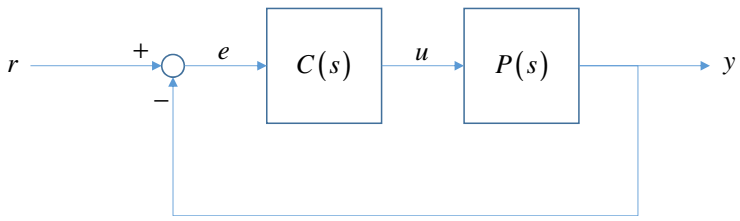


**Fig. 1 Feedback Loop Block Diagram**

The open-loop transfer function obtained for the system broken at any location in the loop in Fig. 1 is given as

$$L(s) = P(s)\,C(s) \tag{1}$$

The sensitivity function $S(s)$ of a feedback system is defined as the closed-loop transfer function from the reference $r$ to the tracking error $e$:

$$S(s) = \frac{E(s)}{R(s)} = \frac{1}{1 + L(s)} \tag{2}$$

where $R(s)$ and $E(s)$ denote the Laplace transforms of the signals $r(t)$ and $e(t)$, respectively. The complementary

sensitivity function $T(s)$ is defined as the closed-loop transfer function from the reference $r$ to the measured output $y$:

$$T(s) = \frac{Y(s)}{R(s)} = 1 - S(s) = \frac{L(s)}{1 + L(s)} \tag{3}$$

where $Y(s)$ denotes the Laplace transform of the signal $y(t)$.

Sensitivity and complementary sensitivity functions govern the overall closed-loop response. Sensitivity function describes the effect of feedback on attenuation of disturbances oscillating with frequency $\omega$. It gives an overview of performance and robustness of a closed-loop system $T(s)$, since it describes variations in the closed-loop system due to perturbation in the open-loop process $L(s)$ as

$$S(s) = \frac{\frac{\Delta T(s)}{T(s)}}{\frac{\Delta L(s)}{L(s)}} = \frac{L(s)}{T(s)} \frac{dT(s)}{dL(s)} \tag{4}$$

The reciprocal of sensitivity magnitude is the Euclidean distance between the critical point $(-1, 0)$ and the Nyquist curve of open-loop transfer function $L(s)$ on the complex plane. The maximum sensitivity magnitude $M_S = \|S(s)\|_\infty = \max_\omega |S(j\omega)|$ is equal to the reciprocal of the vector stability margin which is defined to be the minimum distance to $(-1, 0)$ on the Nyquist plot. Thus, it qualifies as a robustness measure. Provided that the sensitivity peak is known, it can be related to the classical stability margins [27]. Let $GM = -\frac{1}{L(j\omega_{pc})}$ denote the gain margin where $\omega_{pc}$ is the phase crossover frequency such that $\mod\left\{\angle L\left(j\omega_{pc}\right), 360\,\text{deg}\right\} = -180\,\text{deg}$. Also, let $PM = 2\sin^{-1}\left(\frac{1}{2|S(j\omega_{gc})|}\right)$ denote the phase margin where $\omega_{gc}$ is the gain crossover frequency such that $\left|L\left(j\omega_{gc}\right)\right| = 1$. The following inequalities hold between different measures [16, 28].

$$\begin{cases} GM \geq \dfrac{M_S}{M_S - 1} & \text{for gain amplification} \\ GM \leq \dfrac{M_S}{M_S + 1} & \text{for gain reduction} \\ PM \geq 2\sin^{-1}\left(\dfrac{1}{2M_S}\right) \end{cases} \tag{5}$$

### B. Fundamental Properties of Stable Closed-Loop System

*1. Interpolation Constraint*

The closed-loop system is said to be internally stable if all signals in the system remain bounded when a bounded signal is injected at any point in the loop. The transfer function between any two points in the internally stable closed-loop, i.e., all closed-loop sensitivity and complementary sensitivity functions, are stable. Any unstable pole-zero cancellation between the plant and controller results in an unstable closed-loop system, hence, the sensitivity function for an internally stable closed-loop system satisfies the following properties known as the interpolation constraint.

**Lemma 1** (Sensitivity Interpolation Constraint for Internal Stability [1])**.**

Assume that the open-loop transfer function $L(s)$ formed by cascade connection as defined in Eq. (1) is free of any unstable hidden modes. Let $\mathcal{P}_{0+} \triangleq \left\{ p \in \overline{\mathbb{C}}_+ \middle| \ \text{den}(L(p)) = 0 \right\}$ and $\mathcal{Z}_{0+} \triangleq \left\{ z \in \overline{\mathbb{C}}_+ \middle| \ \text{num}(L(z)) = 0 \right\}$ denote the set of poles and zeros of $L(s)$ in the closed RHP, respectively. Also, let $S(s)$ be the sensitivity function defined in Eq. (2). The necessary and sufficient condition for internal stability is as follows:

$$\begin{aligned} & S(s) \text{ is stable} \\ & S(z) = 1, \qquad \forall z \in \mathcal{Z}_{0+} \\ & S(p) = 0, \qquad \forall p \in \mathcal{P}_{0+} \end{aligned} \tag{6}$$

*2. Bode's Sensitivity Integral Formula*

Employing feedback cannot improve performance characteristics uniformly over all frequencies, and thus, control design is always a multi-objective optimisation trading off tracking performance against robustness. One of the fundamental limitations is conventionally described by the following Bode integral of log sensitivity magnitude over the whole frequency range.

**Lemma 2** (Bode Integral Relation for Sensitivity [1, 29])**.**

Let $L(s)$ be a proper rational open-loop transfer function defined in Eq. (1), and $S(s)$ be the sensitivity function defined in Eq. (2). Also, let $\mathcal{P}_+ \triangleq \{ p \in \mathbb{C}_+ | \ \text{den}(L(p)) = 0 \}$ be the set of poles of $L(s)$ in the open RHP. Then, assuming closed-loop stability,

$$\int_0^\infty \ln \left| \frac{S(j\omega)}{S(j\infty)} \right| d\omega = \frac{\pi}{2} \lim_{s \to \infty} \frac{s\left[S(s) - S(\infty)\right]}{S(\infty)} + \pi \sum_{\forall p \in \mathcal{P}_+} p \tag{7}$$

Note that $S(\infty) = 1$ if the relative degree of $L(s)$ is greater than or equal to 1. Also note that the first term in the RHS of Eq. (7) vanishes if $L(s)$ has relative degree greater than or equal to 2. The second term in the RHS of Eq. (7) is a constant in all cases and it vanishes only if the plant is open-loop stable. The relative degree of $L(s)$ is at least 2 in most practical controlled systems as the plant $P(s)$ includes dynamic elements such as actuators and sensors and the controller $C(s)$ typically includes noise filters to enforce sufficient roll-off above certain frequency for reduction of control sensitivity with respect to high-frequency sensor noise. In particular, a controller with nonzero relative degree is adopted for elastic systems because relative degree zero controllers with infinite bandwidth may excite structural flexibility modes.

When $L(s)$ has relative degree greater than or equal to 2, Eq. (7) behaves like an area conservation law since the integral value is a constant regardless of the controller mapping. The conservation law interpretation of Lemma 2 indicates that i) low-frequency sensitivity reduction always induces high-frequency penalty, and ii) open-loop unstable plants are inherently more sensitive than open-loop stable plants.

## III. Approximation of Achievable Open-Loop Frequency Response

The sensitivity function for a stable closed-loop system exhibits several inherent algebraic properties including the relations discussed in Sec. II.B. From the view of controller design, the fundamental *properties* of a stable closed-loop system can conversely interpreted as the fundamental *constraints* that should be satisfied by every stabilising controller. This observation motivates the proposed method in which a desired sensitivity function satisfying the constraints is constructed so that it can be realised with a controller admissible for the given plant.

To highlight the key ideas more clearly, this section first develops the method for minimum-phase plants based on direct inversion of constructed desired sensitivity, since the proposed method in this case involves only simple algebra. The discussion is followed by the method for nonminimum-phase plant case based on approximate inversion by using the approach developed in [3–5] for minimisation of weighted sensitivity.

### A. Ideal Sensitivity Magnitude Prototype

For many realistic $L(s)$ of relative degree not less than 2, sensitivity reduction in a low-frequency band for improved disturbance rejection and reference tracking inevitably entails sensitivity amplification in a high-frequency region as witnessed by the Bode integral conservation law in Eq. (7). In these practical systems, the optimal controller as evaluated according to $\|S(s)\|_\infty$ is the transfer function such that $|S(j\omega)|$ is a constant for all frequencies where $|S(j\omega)| > 1$. That is, the maximum robustness of the loop is likely to be attained by spreading the amount of sensitivity reduced in the low-frequency region uniformly over the rest high-frequency region so that the sacrifice in high-frequency attenuation is minimised. Minimisation of the sensitivity peak $M_S$ is a design strategy addressed in [3, 6] to achieve maximal robustness evaluated in terms of vector stability margin, which is one of the robustness measures described in Sec. II.A.

The Bode sensitivity integral is an improper integral over a semi-infinite interval, hence the ideal strategy may leverage entire frequency range to avoid sensitivity amplification. However, $M_S$ cannot be arbitrarily minimised since any feedback control system in practice is constrained by bandwidth limitations imposed due to the physical hardware. The bandwidth of each hardware component comprising the control loop, modelling inaccuracies, and sensor noise all limit achievable closed-loop bandwidth. The hardware bandwidth limitations confines the region allowed for inevitable sensitivity amplification to a finite interval below certain frequency associated with the minimum among the bandwidths of various physical elements in the loop. The limit frequency once referred to as the *available bandwidth* in [2] is the frequency $\omega_a$ such that

$$\int_{\omega_a}^{\infty} \ln |S(j\omega)| \, d\omega \approx 0 \tag{8}$$

is a reasonable approximation. Note that the available bandwidth is different from the frequency at which the closed-loop gain curve crosses $-3$dB and its value is almost purely a matter of the plant hardware.

Consider a plant of which the unstable pole locations and the available bandwidth are well known. Let $\omega_L$ be the

cutoff frequency up to which good reference tracking and disturbance attenuation is desired. In practice, $\omega_L$ is lower bounded by the rise time constraint. Then, the sensitivity magnitude distribution shown in Fig. 2a can be regarded an ideal sensitivity magnitude prototype and it can be expressed as

$$|S_{\text{ideal}}(j\omega)| = \begin{cases} M_S \frac{\omega}{\omega_L} & \text{for } \omega \leq \omega_L \\ M_S & \text{for } \omega_L \leq \omega \leq \omega_a \\ 1 & \text{for } \omega \geq \omega_a \end{cases} \tag{9}$$

Substituting Eq. (9) into Eq. (7) and applying the approximation given by Eq. (8), we have

$$\int_0^{\omega_L} \ln\left(M_S \frac{\omega}{\omega_L}\right) d\omega + (\omega_a - \omega_L) \ln M_S \approx \pi \sum_{\forall p \in \mathcal{P}_+} p \tag{10}$$

Solving Eq. (10) for $M_S$ yields an approximation for the sensitivity peak as

$$M_S \approx \exp\left(\frac{\omega_L + \pi \sum_{\forall p \in \mathcal{P}_+} p}{\omega_a}\right) \tag{11}$$

Stability margin requirements can be verified by substituting the approximate sensitivity peak given by Eq. (11) into the basic inequality relation given as Eq. (5), however, one can draw only a conservative hence hardly meaningful conclusion with this test.

### B. Desired Sensitivity Function

Magnitude of the sensitivity function of a real-world feedback system cannot have a sharp-edged shape showing sudden change at certain breakpoints as shown in Fig. 2a. Also, Eq. (9) and Fig. 2a represent only the magnitude information of the sensitivity. Therefore, a sensitivity function including its phase should be constructed as a transfer function that is *realisable* for the given plant with a proper rational stabilising controller of a modest order so that its magnitude closely approximates the profile given by Eq. (9).

A sensitivity profile should satisfy the structural constraints for it to be realisable through feedback. The conditions that should be considered in the elementwise construction of the *desired* sensitivity function $S_{\text{desired}}(s)$ are as follows:

- Condition (1) Magnitude: $|S_{\text{desired}}(j\omega)|$ should be close to $|S_{\text{ideal}}(j\omega)|$.
- Condition (2) Closed-Loop Internal Stability: Eq. (6) should be satisfied, and all poles of $S_{\text{desired}}(s)$ should be located on the LHP.
- Condition (3) High-Frequency Roll-Off: $S_{\text{desired}}(\infty) = 1$ should be satisfied so that the corresponding open-loop transfer function $L_{\text{approx}}(s)$ rolls off as $\omega \to \infty$. That is, the relative degree of $S_{\text{desired}}(s)$ should be 0, and the highest order coefficients of its denominator should be equal to that of its numerator.

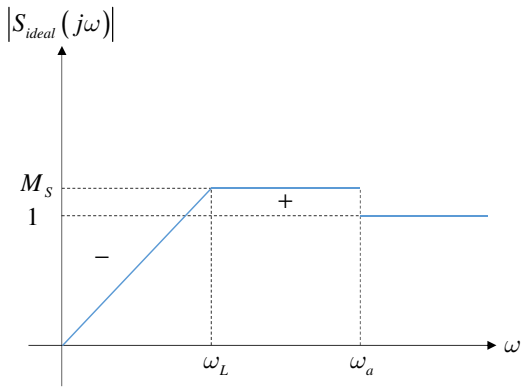


**(a) Ideal Sensitivity Magnitude Prototype**

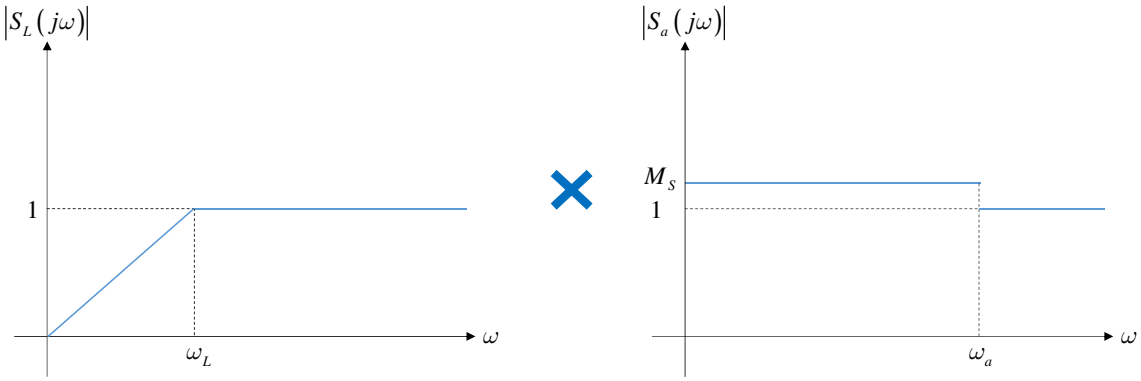


**(b) Decomposition of Ideal Sensitivity Magnitude Prototype**

**Fig. 2 Construction of Ideal Sensitivity Magnitude Prototype**

- Condition (4) Integral-like Action: $S_{\text{desired}}(0) \approxeq 0$ should be satisfied so that the corresponding open-loop transfer function $L_{\text{approx}}(s)$ has an integrator-like element $\frac{1}{s+\varepsilon}$ with $0 \leq \varepsilon \ll 1$ as a factor.
- Condition (5) Low Order: $S_{\text{desired}}(s)$ of a reasonably low order is preferable since a low-order controller is more realistic in practice.

Given that $L(s)$ is a rational transfer function, a desired sensitivity function $S_{\text{desired}}(s)$ can be constructed by combination of multiple factors, each responsible for its own physical role. Decomposition of the ideal sensitivity magnitude prototype as shown in Fig. 2b provides the asymptotes for the factors. Numerical fitting of a transfer function to the magnitude-only frequency response data for the ideal prototype given in Eq. (9) is also an option as long as the constraint satisfaction is guaranteed, but this approach is not taken for the purpose of this study.

The following sections address construction of the desired sensitivity function which plays a central role in approximation of the robustness bound. The construction procedure depends on the presence of RHP zeros in the plant. Section III.B.1 considers minimum-phase plants while requiring the open-loop transfer function to have a relative degree greater than or equal to 2. Section III.B.2 develops a method for nonminimum-phase plants with the constraint imposed

on the open-loop transfer function that it has a relative degree greater than or equal to 1.

*1. Case 1. Minimum-Phase Plant: Inversion of Desired Sensitivity Function*

The interpolation constraint described in Lemma 1 implies that the desired sensitivity function $S_{\text{desired}}(s)$ for minimum-phase plants can be factored as

$$S_{\text{desired}}(s) = S_{MP}(s)\, B_p(s) \tag{12}$$

where $B_p(s)$ represents the Blaschke product given by

$$B_p(s) = \begin{cases} 1 & \text{if } \mathcal{P}_+ = \emptyset \\ \displaystyle\prod_{\forall p \in \mathcal{P}_+} \frac{s-p}{s+\overline{p}} & \text{if } \mathcal{P}_+ \neq \emptyset \end{cases} \tag{13}$$

In Eq. (12), $S_{MP}(s)$ represents the minimum-phase component which is a stable rational function having no zeros in the open RHP and no poles in the finite closed RHP. Another term $B_p(s)$ is an stable all-pass function which contributes only to the phase variations of the sensitivity function, i.e., $\left|B_p(j\omega)\right| = 1, \forall\omega$.

Putting together the above discussions, a desired sensitivity profile can be composed as

$$\begin{aligned} S_{\text{desired}}(s) &= S_L(s)\, S_a(s)\, B_p(s) \\ &= \frac{s+\epsilon}{s+\omega_L} \frac{s^2 + \sqrt{2}\omega_a s + {\omega_a}^2}{s^2 + \sqrt{2}\omega_c s + {\omega_c}^2} \prod_{\forall p \in \mathcal{P}_+} \frac{s-p}{s+\overline{p}} \end{aligned} \tag{14}$$

where $0 \leq \epsilon \ll 1$ and $\omega_c < \omega_a$. In Eq. (14), the first factor $S_L(s)$ contributes to sensitivity reduction in the low-frequency region, the second factor $S_a(s)$ makes the sensitivity magnitude decrease close to 1 at the frequencies higher than the available bandwidth $\omega_a$, and the last factor $B_p(s)$ models the nonminimum-phase variations of sensitivity due to the unstable poles of the open-loop plant. The log magnitude of a product is the sum of log magnitudes, hence, the structure given by Eq. (14) forms the backbone of a desired sensitivity function that resembles the log magnitude prototype as shown in Fig. 2b. The performance goal for control design gives the cutoff frequency $\omega_L$, the physical properties of the plant determines the unstable plant poles $p \in \mathcal{P}_+$ and the available bandwidth $\omega_a$, and Eq. (14) specifies the form of the realisable sensitivity function.

The remaining coefficient $\omega_c$ in Eq. (14) can then be determined by enforcing relative degree no less than 2 for the corresponding open-loop transfer function $L(s)$, since it is usual in many practical systems as discussed in Sec. II.B.2.

The sensitivity function defined by Eq. (2) can be rewritten as

$$S(s) = \frac{\text{den}(L(s))}{\text{den}(L(s)) + \text{num}(L(s))} \tag{15}$$

Equation (15) clearly shows that the first and second highest order coefficients of $\text{den}(S(s))$ and $\text{num}(S(s))$ are identical to each other, respectively, when the relative degree of $L(s)$ is greater than or equal to 2. Thus, the coefficient $\omega_c$ can be determined by equating the highest order coefficients of $\text{den}(S(s))$ and $\text{num}(S(s))$.

Suppose that the plant has $N$ unstable poles. Equation (14) can be expanded as

$$\begin{aligned} S_{\text{desired}}(s) &= \frac{s^3 + \left(\epsilon + \sqrt{2}\omega_a\right) s^2 + \left({\omega_a}^2 + \sqrt{2}\epsilon\omega_a\right) s + \epsilon{\omega_a}^2}{s^3 + \left(\omega_L + \sqrt{2}\omega_c\right) s^2 + \left({\omega_c}^2 + \sqrt{2}\omega_L\omega_c\right) s + \omega_L{\omega_c}^2} \frac{s^N - \sum_{i=1}^{N} p_i s^{N-1} + \cdots}{s^N + \sum_{i=1}^{N} \overline{p}_i s^{N-1} + \cdots} \\ &= \frac{s^{N+3} + \left(\epsilon + \sqrt{2}\omega_a - \sum_{i=1}^{N} p_i\right) s^{N+2} + \cdots}{s^{N+3} + \left(\omega_L + \sqrt{2}\omega_c + \sum_{i=1}^{N} \overline{p}_i\right) s^{N+2} + \cdots} \end{aligned} \tag{16}$$

By satisfying the relation $\epsilon + \sqrt{2}\omega_a - \sum_{i=1}^{N} p_i = \omega_L + \sqrt{2}\omega_c + \sum_{i=1}^{N} \overline{p}_i$ , $\omega_c$ can be determined as

$$\omega_c = \omega_a - \frac{\omega_L - \epsilon + \sum_{i=1}^{N} \left(p_i + \overline{p}_i\right)}{\sqrt{2}} = \omega_a - \frac{\omega_L - \epsilon + 2 \sum\limits_{\forall p \in \mathcal{P}_+} p}{\sqrt{2}} \tag{17}$$

*2. Case 2. Nonminimum-Phase Plant: Approximate Inversion of Desired Sensitivity Function*

When the open-loop plant has at least one zero in the RHP, the open-loop transfer function cannot simply be obtained by inverting the desired sensitivity function constructed for minimum-phase plants because the exact inverse entails cancellation of unstable plant zero with unstable controller pole. Only approximate inversion is available for nonminimum-phase plants. To deal with nonminimum-phase plants, this study utilises the weighted sensitivity optimisation approach developed in [5] for minimisation of $\|W(s) S(s)\|_\infty$ where $W(s)$ is a weighting function. Readers are referred to [5] for full discussion of the details about the weighted sensitivity optimisation approach.

Suppose that the nonminimum-phase plant has neither poles nor zeros on the imaginary axis and the zeros are distinct. Let the given weighting function $W(s)$ and its inverse are both stable. The method of [5] gives a formula for computing the optimal weighted sensitivity function when the RHP zeros $z_i \in \mathcal{Z}_+ \triangleq \{z \in \mathbb{C}_+ | \ \text{num}(L(z)) = 0\}$ of

$P(s)$ are distinct. As the first step, define the associated matrices as

$$\begin{aligned} M &= \left[M_{ij}\right] = \frac{1}{z_i + \overline{z}_j} \\ T &= \left[T_{ii}\right] = \operatorname{diag}\left[\frac{W(z_i)}{B_p(z_i)}\right] \\ N &= TM \end{aligned} \tag{18}$$

where $B_p(s)$ is the Blaschke product defined in Eq. (13). The Hermitian and positive definite matrix $M$ has a factorisation $M = U^*U$ which enables the transformation $x = U\xi$. The original problem of minimising the norm of weighted sensitivity reduces to the problem of finding the maximum eigenvalue and the associated eigenvector as shown below

$$\begin{aligned} \tilde{x} &= \arg\max_x \left\{x^*N^*M^{-1}Nx : x^*Mx = 1\right\} \\ &= U^{-1} \arg\max_\xi \left\{\xi^*UT^*U^{-1}\left(UT^*U^{-1}\right)^*\xi : \xi^*\xi = 1\right\} \\ &= U^{-1}\phi_{\lambda_{\max}}\left(UT^*U^{-1}\left(UT^*U^{-1}\right)^*\right) \\ \tilde{y} &= M^{-1}N\tilde{x} = M^{-1}TM\tilde{x} \end{aligned} \tag{19}$$

where $\phi_{\lambda_{\max}}(X)$ denotes the eigenvector associated with the maximum eigenvalue of $X$. According to [5], the minimum weighted sensitivity norm solution $S_{\text{optimal}}(s)$ can be represented as

$$S_{\text{optimal}}(s) = W^{-1}(s) B_p(s) \frac{\sum_i \tilde{y}_i K_i(s)}{\sum_i \tilde{x}_i K_i(s)} \tag{20}$$

where $K_i(s) \triangleq \frac{1}{s+\overline{z}_i}, \forall z_i \in \mathcal{Z}_+$.

In particular, the set of expressions presented in Eqs. (18)-(20) reduces to a single equation for the optimal sensitivity function in the special case when the plant has one positive real zero. With all the intermediate steps becoming scalar operations, the optimal sensitivity function can be represented as

$$S_{\text{optimal}}(s) = \frac{W^{-1}(s) B_p(s)}{W^{-1}(z) B_p(z)} \tag{21}$$

It is obvious from the expression that $S_{\text{optimal}}(s)$ in Eq. (21) satisfies the interpolation constraint given by Eq. (6), i.e., $S_{\text{optimal}}(p \in \mathcal{P}_+) = 0$ and $S_{\text{optimal}}(z \in \mathcal{Z}_+) = 1$, regardless of the choice of $W(s)$.

Motivated by the descriptions above, one can construct the desired sensitivity function by taking the structure of optimal solution shown in Eqs. (20) or (21). For simplicity of further development, suppose that the plant has a single

positive real zero at $z$. Let us take the weighting function as

$$W(s) = \{S_L(s) S_a(s)\}^{-1} \tag{22}$$

where $S_L(s)$ and $S_a(s)$ have the same form as those given in Eq. (14). The above choice of weighting function is to encode the shape of the desired sensitivity magnitude, since the magnitude of optimal sensitivity function is inversely proportional to that of the weighting function as shown in Eq. (20). Then, the desired sensitivity function can be specified as

$$S_{\text{desired}}(s) = \frac{S_L(s) S_a(s) B_p(s)}{S_L(z) S_a(z) B_p(z)} \tag{23}$$

The parameters $\omega_L$, $\epsilon$ in $S_L(s)$, and $\omega_a$ in $S_a(s)$ are all given by the performance requirements and the physical hardware characteristics. The remaining coefficient $\omega_c$ in Eq. (23) can be determined in a similar manner to the minimum-phase plant case by specifying the minimum relative degree of the open-loop transfer function $L(s)$. However, it is difficult to solve for the value of $\omega_c$ guaranteeing the relative degree of open-loop transfer function to be at least 2 by equating the first two highest order coefficients in the denominator and the numerator of $S_{\text{desired}}(s)$. Instead, the remaining parameter $\omega_c$ can be determined to satisfy $S_{\text{desired}}(\infty) = 1$ so that the corresponding open-loop transfer function $L(s)$ has relative degree no less than 1. It is obvious from Eq. (23) that the condition $S_{\text{desired}}(\infty) = 1$ is equivalent to

$$S_L(z) S_a(z) B_p(z) = \frac{z+\epsilon}{z+\omega_L} \frac{z^2 + \sqrt{2}\omega_a z + {\omega_a}^2}{z^2 + \sqrt{2}\omega_c z + {\omega_c}^2} \prod_{\forall p \in \mathcal{P}_+} \frac{z-p}{z+\overline{p}} = 1 \tag{24}$$

because $S_L(\infty) S_a(\infty) B_p(\infty) = 1$. Equation (24) is a quadratic equation in $\omega_c$, thus, its solution can be obtained as

$$\omega_c = \frac{-\sqrt{2}z + \sqrt{4\left(z^2 + \sqrt{2}\omega_a z + {\omega_a}^2\right) S_L(z) B_p(z) - 2z^2}}{2} \tag{25}$$

### C. Achievable Open-Loop Transfer Function

Suppose that all the parameters in $S_{\text{desired}}(s)$ are specified and it satisfies the interpolation constraint for closed-loop internal stability as described in Lemma 1. The open-loop transfer function can be obtained by inversion as

$$L_{\text{approx}}(s) = \frac{1}{S_{\text{desired}}(s)} - 1 \tag{26}$$

The open-loop frequency response with the best achievable robustness can be approximated by $L_{\text{approx}}(j\omega)$. The estimates for the maximum stability margins can be obtained by drawing Bode or Nyquist diagrams and taking the values arising from crossover points near the frequency mainly associated with the controller, namely, the cutoff frequency $\omega_L$.

## IV. Examples

This section presents analysis examples to illustrate the effectiveness of the proposed method in approximating the best achievable stability margins. The short-period mode longitudinal dynamics model for a statically unstable missile is considered. The proposed method is applied to the analysis of pitch angular rate and normal acceleration controllers which are usually formulated as SISO design problems in missile autopilots [30–34]. Case 1 deals with pitch rate control loop as an application to a minimum-phase plant, and Case 2 addresses the normal acceleration controller to test the method on a nonminimum-phase plant. The rough estimates obtained by the proposed method are compared with the results of mixed-sensitivity $\mathcal{H}_\infty$ optimisation which can be taken as the optimally robust solution to support the validity.

### A. Short-Period Mode Longitudinal Dynamics

Assuming that the roll control response is sufficiently fast and the missile is effectively an axisymmetric body so that the motion in the pitch plane can be decoupled from the other axes, the short-period mode of the rigid body longitudinal dynamics can be represented as follows:

$$\begin{bmatrix} \dot{\alpha} \\ \dot{q} \end{bmatrix} = \begin{bmatrix} Z_\alpha & 1 \\ M_\alpha & M_q \end{bmatrix} \begin{bmatrix} \alpha \\ q \end{bmatrix} + \begin{bmatrix} Z_\delta \\ M_\delta \end{bmatrix} \delta \tag{27}$$
$$a_z = V\left(Z_\alpha \alpha + Z_\delta \delta\right)$$

where $\alpha$, $q$, $V$, $a_z$, and $\delta$ denote the angle-of-attack, the body angular rate, the speed, the normal acceleration, and the control surface deflection, respectively, and the components of the system matrices are the dimensional derivatives. The transfer functions that map the control surface deflection to the body angular rate and the normal acceleration are given as

$$P_q(s) = \frac{q(s)}{\delta(s)} = \frac{b_1 s + b_0}{s^2 + a_1 s + a_0}, \qquad P_a(s) = \frac{a_z(s)}{\delta(s)} = \frac{c_2 s^2 + c_1 s + c_0}{s^2 + a_1 s + a_0} \tag{28}$$

where $a_1 = -Z_\alpha - M_q$, $a_0 = M_q Z_\alpha - M_\alpha$, $b_1 = M_\delta$, $b_0 = M_\alpha Z_\delta - Z_\alpha M_\delta$, $c_2 = V Z_\delta$, $c_1 = -V Z_\delta M_q$, and $c_0 = -V b_0$. Also, a linear second-order model is considered for the actuator dynamics as

$$P_{\text{act}}(s) = \frac{\delta(s)}{\delta_{\text{cmd}}(s)} = \frac{{\omega_{\text{act}}}^2}{s^2 + 2\zeta_{\text{act}}\omega_{\text{act}} s + {\omega_{\text{act}}}^2} \tag{29}$$

where $\delta_{\text{cmd}}$ denotes the commanded control surface deflection, $\zeta_{\text{act}}$ is the damping ratio, and $\omega_{\text{act}}$ is the natural frequency of the actuator model. The overall plant is given by the aggregation of the bare airframe and the actuator as

$$P(s) = P_i(s)\, P_{\text{act}}(s) \tag{30}$$

where $i = q$ in Case 1 and $i = a$ in Case 2.

The model data borrowed from [32] are summarised in Table 1. A linear model for the airframe short-period mode of the longitudinal dynamics typically includes a pair of lightly damped complex conjugate poles (for the open-loop stable airframe) or a pair of real-axis poles of comparable magnitude with one in the RHP (for the open-loop unstable airframe). Recent tactical missile designs allow intentional relaxation of static stabilities for higher manoeuvrability and wider flight envelope. The model used is statically unstable since $M_\alpha > 0$ as shown in Table 1, and it has one unstable pole at $s = 6.4212$. Moreover, the pitch rate plant transfer function $P_q(s)$ has a zero at $s = -0.6583$ which is in the LHP but quite close to the origin, posing difficulties in angular rate stabilisation with a simple proportional feedback. On the other hand, the normal acceleration plant transfer function $P_a(s)$ has a RHP zero at $s = 23.41$.

**Table 1 Simulation Model Data**

| Parameters | Unit | Value | Parameters | Unit | Value |
|---|---|---|---|---|---|
| $V$ | m/s | 40 | $M_q$ | $\mathrm{s}^{-1}$ | $-0.7$ |
| $Z_\alpha$ | $\mathrm{s}^{-1}$ | $-0.6$ | $M_\delta$ | $\mathrm{s}^{-2}$ | $-30$ |
| $Z_\delta$ | $\mathrm{s}^{-1}$ | $-0.035$ | $\omega_{\mathrm{act}}$ | Hz | 20 |
| $M_\alpha$ | $\mathrm{s}^{-2}$ | 50 | $\zeta_{\mathrm{act}}$ | – | $\frac{1}{\sqrt{2}}$ |

### B. Comparison with Minimum Sensitivity $\mathcal{H}_\infty$ Synthesis Results

This study considers the result of mixed-sensitivity $\mathcal{H}_\infty$ loop shaping as the reference to assess how well the proposed method approximates the best practicable stability margins. The optimal design problem is formulated as follows:

$$\begin{aligned} &\text{minimise} && \left\| \begin{matrix} W_1(s)\, S(s) \\ W_2(s)\, C(s)\, S(s) \end{matrix} \right\|_\infty \\ &\text{subject to} && C(s) \text{ stabilises closed-loop} \end{aligned} \tag{31}$$

where $W_1(s)$ and $W_2(s)$ are the weights on the sensitivity and the control sensitivity, respectively. The result of optimisation substantially depends on the choice of weighting functions. Two different types of control sensitivity weights $W_2(s)$, namely, a constant and a high frequency cutoff filter, are considered for the comparison purpose. The natural frequency of the actuator is considered as the available bandwidth to simply consider the physical actuation limit. The control design requirements, the available bandwidth, and the weighting functions are summarised in Table 2. The `mixsyn` function which makes use of the `hinfsyn` function included in the MATLAB Robust Control Toolbox is utilised for the mixed-sensitivity $\mathcal{H}_\infty$ synthesis with the solution algorithm based on linear matrix inequalities.

**Table 2 Control Design Specifications**

| Parameters | Unit | Case 1 | Case 2 |
|---|---|---|---|
| $\omega_L$ | Hz | 5 | 2 |
| $\omega_a$ | Hz | $\omega_{\text{act}}$ | $\omega_{\text{act}}$ |
| $\epsilon$ | – | 0 | $10^{-4}$ |
| $W_1(s)$ | – | $\frac{s+\omega_L}{s+10^{-4}}$ | $\frac{s+\omega_L}{s+\epsilon}$ |
| $W_2(s)$ | – | Case 1-1: 1 | Case 2-1: 2 |
| | – | Case 1-2: $10\frac{s+\omega_a}{s+20\omega_a}$ | Case 2-2: $2\frac{s+\omega_a}{s+2\omega_a}$ |

*1. Case 1. Minimum-Phase Plant: Analysis for Pitch Rate Control*

The example Case 1 considers pitch rate controller analysis to demonstrate the proposed method for minimum-phase plants. Figures 3-6 show the Bode magnitude diagram of sensitivity function, the Bode and Nyquist diagrams of open-loop frequency response, and the Bode diagram of closed-loop frequency response, respectively, for Case 1. Figure 7 shows the time-domain characteristics with closed-loop step response. Also, the frequency-domain response characteristics for Case 1 are shown in Table 3. Comparison between the open-loop and the closed-loop frequency responses for the proposed approximation method and their respective counterparts obtained from numerical optimisation shows the remarkable similarity of the overall trend. In particular, the approximate result closely matches the optimal synthesis results for both Cases 1-1 and 1-2 around the frequency $\omega_L$ which is mainly associated with the controller's nominal performance as it is close to the gain crossover frequencies shown in Table 3. Table 3 shows that the stability margins and the associated crossover frequencies are also accurate enough to be used as reasonable estimates. Overall, the results support the validity of the proposed method for minimum-phase plants based on sensitivity inversion in estimating the best achievable robustness properties.

**Table 3 Open-Loop and Closed-Loop Frequency Response Characteristics (Case 1)**

| Indices | Unit | Approximation | $\mathcal{H}_\infty$ Synthesis - Case 1-1 | $\mathcal{H}_\infty$ Synthesis - Case 1-2 |
|---|---|---|---|---|
| Gain Margin $GM$ | dB | −12.8282, 13.1263 | −12.0216, 12.8860 | −12.7564, 12.6260 |
| Phase Crossover Frequency $\omega_{GM}$ | Hz | 0.8463, 17.2291 | 1.0522, 18.9509 | 0.8645, 19.2736 |
| Phase Margin $PM$ | deg | 49.1795 | 48.3940 | 51.6289 |
| Gain Crossover Frequency $\omega_{PM}$ | Hz | 4.6328 | 4.6734 | 4.7004 |
| Delay Margin $DM$ | s | 0.0295 | 0.0288 | 0.0305 |
| Closed-Loop Bandwidth $\omega_{BW}$ | Hz | 9.6635 | 9.5754 | 9.4897 |

*2. Case 2. Nonminimum-Phase Plant: Analysis for Normal Acceleration Control*

The example Case 2 considers normal acceleration controller analysis to demonstrate the proposed method for nonminimum-phase plants. Note that the main purpose of this example is to test the validity in nonminimum-phase case while dealing with the analysis of SISO control of $P_a(s)$ without considering the successive loop closure structure. Figures 8-11 show the results of Case 2 with the Bode magnitude diagram of sensitivity function, the Bode and Nyquist diagrams of open-loop frequency response, and the Bode diagram of closed-loop frequency response, respectively. Figure 12 shows the closed-loop step response. Also, Table 4 lists the frequency-domain response characteristics for each entity considered in Case 2. Comparison between the results of the proposed approximation method and the numerical optimisation method shows similarities as well as differences in their frequency response characteristics. In a similar manner to Case 1, the approximation method yields a sensitivity magnitude that is close to the results of optimal synthesis for Cases 2-1 and 2-2 mainly in the low-frequency region around $\omega_L$. Consequently, the stability margins and the crossover frequencies obtained from approximation are quite close to the optimisation results in Table 4, except the gain margin at the higher phase crossover frequencies. However, the responses show discrepancies in the higher frequency region which can be attributed mainly to the fact that parameter $\omega_c$ determined as in Eq. (25) only guarantees relative degree of $L(s)$ to be no less than 1. The relative degree of $L(s)$ governs the slope of high-frequency roll-off in $|L(j\omega)|$, hence, the observed discrepancies in the high-frequency trends can be reduced if the relative degree of $L(s)$ becomes no less than 2. Despite this limitation in higher frequency region, the simulation results support the usefulness of the proposed method for nonminimum-phase plants based on approximate sensitivity inversion in estimating the achievable stability margins in the low-frequency region around $\omega_L$.

**Table 4 Open-Loop and Closed-Loop Frequency Response Characteristics (Case 2)**

| Indices | Unit | Approximation | $\mathcal{H}_\infty$ Synthesis - Case 2-1 | $\mathcal{H}_\infty$ Synthesis - Case 2-2 |
|---|---|---|---|---|
| Gain Margin $GM$ | dB | −5.6566, 3.6434 | −5.6250, 4.1627 | −5.8546, 3.8066 |
| Phase Crossover Frequency $\omega_{GM}$ | Hz | 0.6959, 7.6289 | 0.6844, 9.7585 | 0.6990, 10.3220 |
| Phase Margin $PM$ | deg | 22.7731 | 23.8268 | 24.0936 |
| Gain Crossover Frequency $\omega_{PM}$ | Hz | 2.3732 | 2.3064 | 2.4459 |
| Delay Margin $DM$ | s | 0.0267 | 0.0287 | 0.0274 |
| Closed-Loop Bandwidth $\omega_{BW}$ | Hz | 19.8629 | 35.0576 | 38.6402 |

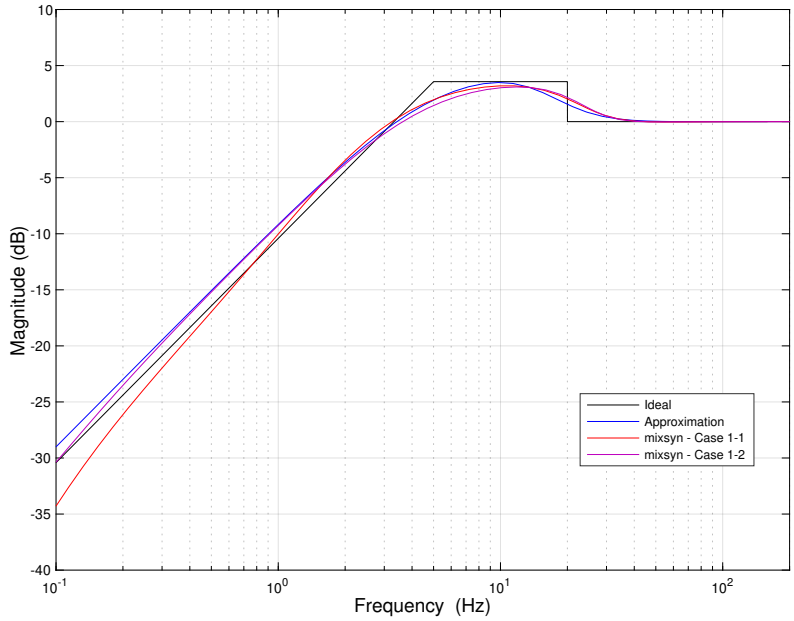


**Fig. 3 Log-Magnitude of Sensitivity Frequency Response $20\log_{10}|S(j\omega)|$ (Case 1)**

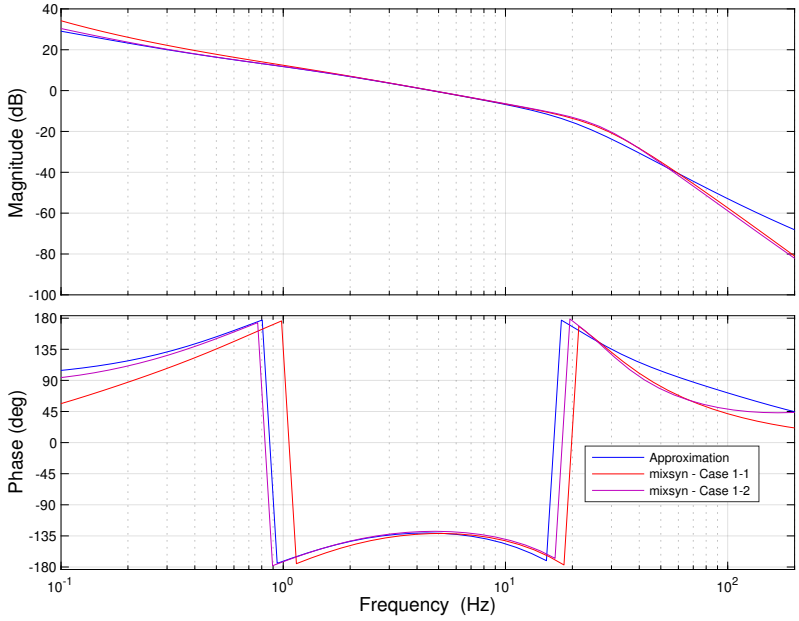


**Fig. 4 Bode Diagram of Open-Loop Frequency Response $L(j\omega)$ (Case 1)**

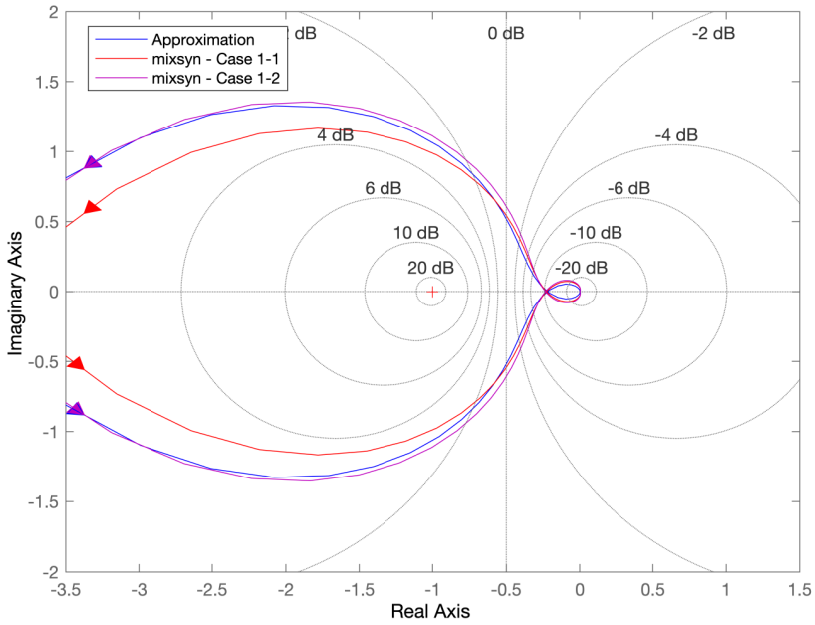


**Fig. 5 Nyquist Diagram of Open-Loop Frequency Response $L(j\omega)$ (Case 1)**

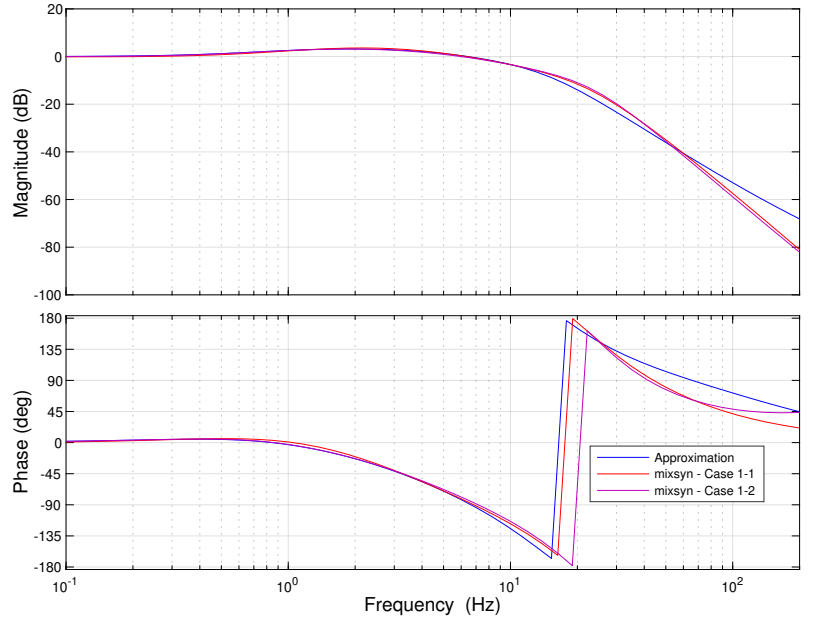


**Fig. 6 Bode Diagram of Closed-Loop Frequency Response $T(j\omega)$ (Case 1)**

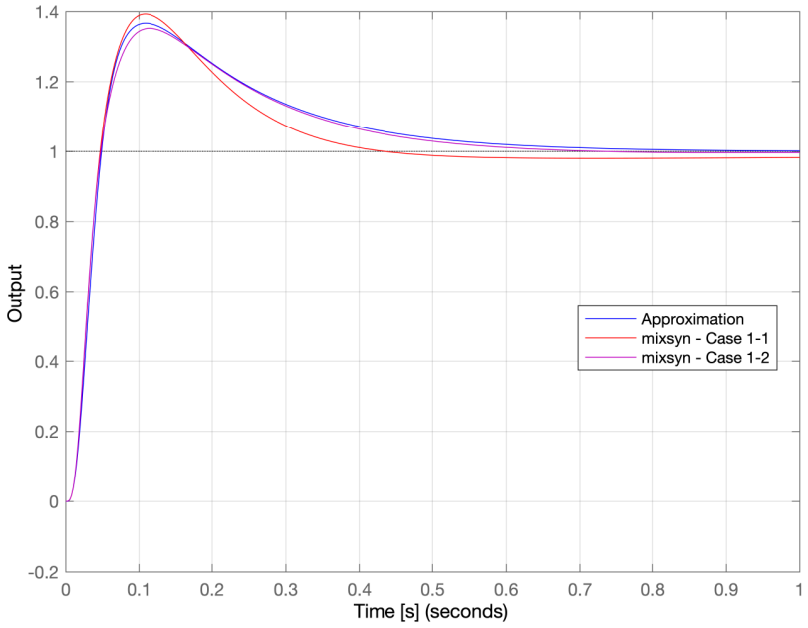


**Fig. 7 Step Response of Closed-Loop System $T(s)$ (Case 1)**

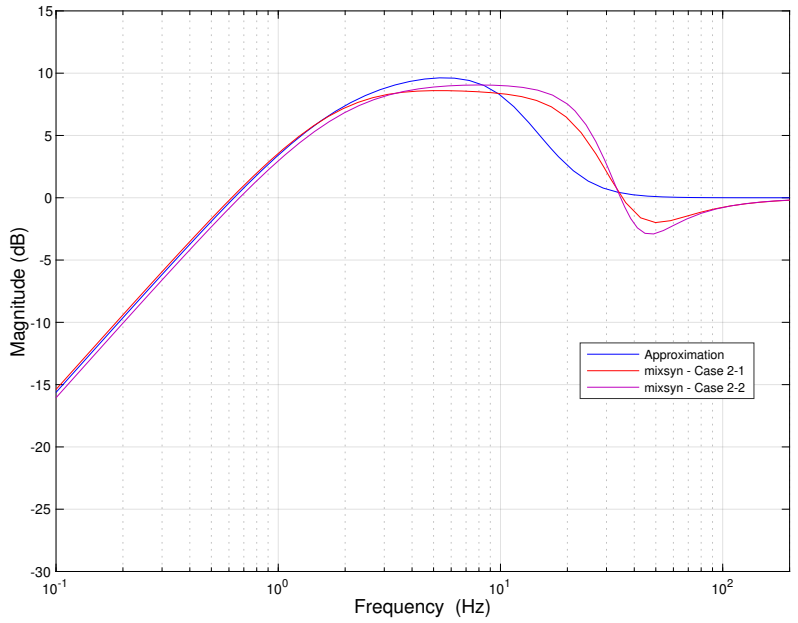


**Fig. 8 Log-Magnitude of Sensitivity Frequency Response $20\log_{10}|S(j\omega)|$ (Case 2)**

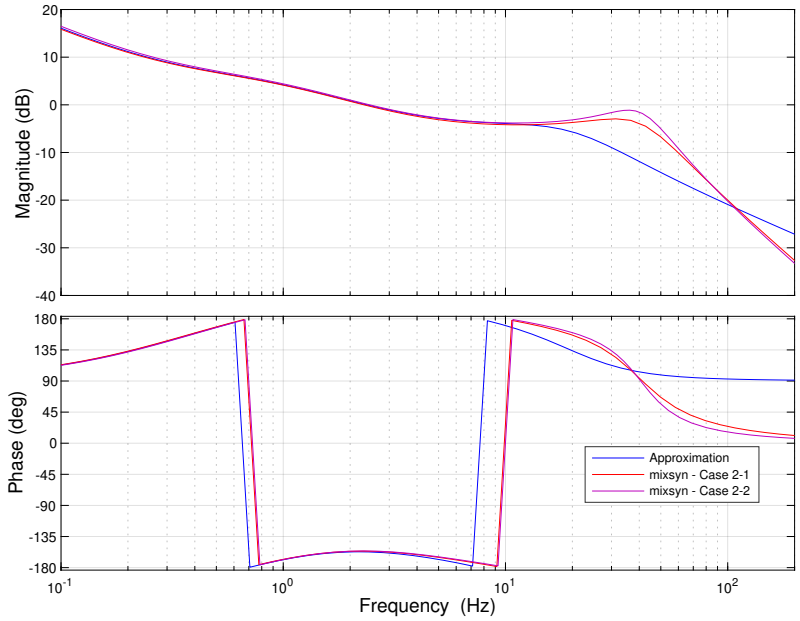


**Fig. 9 Bode Diagram of Open-Loop Frequency Response $L(j\omega)$ (Case 2)**

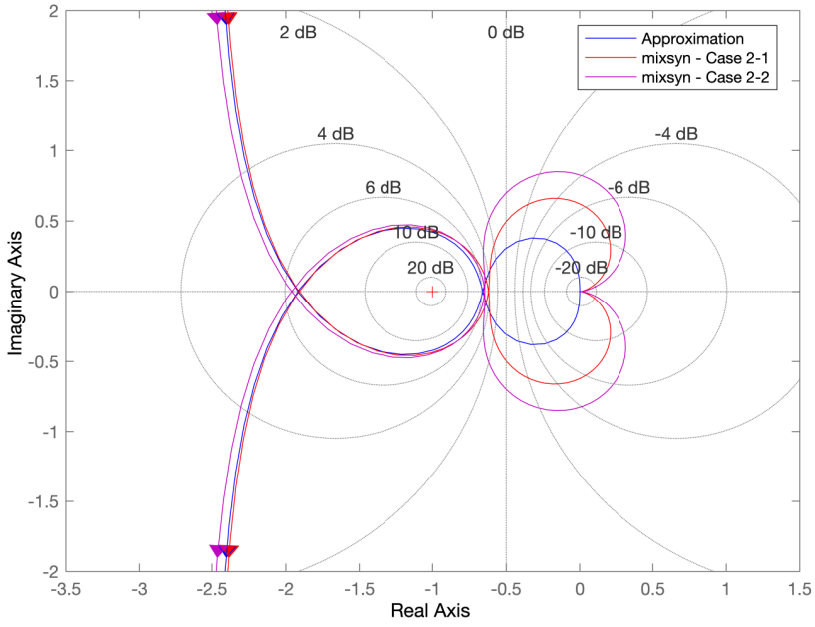


**Fig. 10 Nyquist Diagram of Open-Loop Frequency Response $L(j\omega)$ (Case 2)**

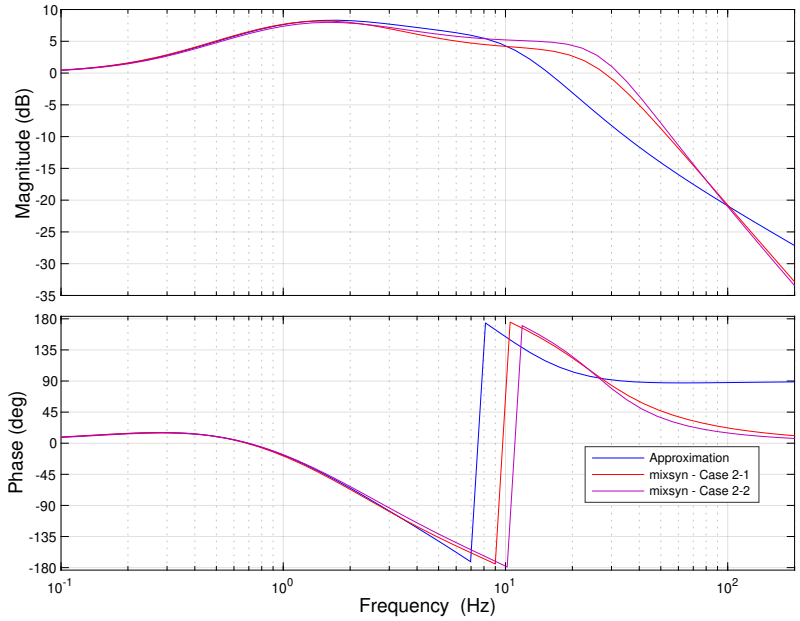


**Fig. 11 Bode Diagram of Closed-Loop Frequency Response $T(j\omega)$ (Case 2)**

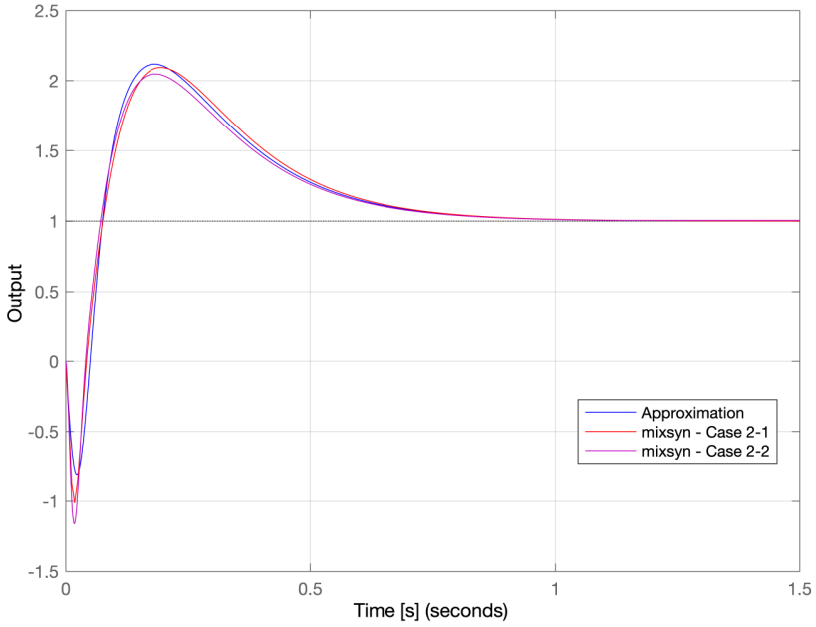


**Fig. 12 Step Response of Closed-Loop System $T(s)$ (Case 2)**

## V. Conclusions

This Note presented a method to approximate the achievable robustness limit for a given plant based on inversion of a realisable sensitivity function. The proposed method is centred around the desired sensitivity function which is purposely constructed to respect several structural constraints that are always satisfied by a sensitivity function for an internally stable closed-loop system. The engineering simplifications were discussed in the review of the Bode's sensitivity integral conservation constraint. The numerical analysis examples which address control of pitch rate and normal acceleration for a statically unstable missile demonstrated that the proposed method provides estimates for the achievable classical stability margins that are comparable to the numerical optimal solution. The proposed approximation procedure focuses only on the relative stability as measured with the frequency-domain response while not paying much concern on the time-domain response characteristics, hence, a controller designed to achieve certain balance between performance and robustness may possess smaller stability margins than the estimated achievable robustness limit. In this respect, the largest achievable stability margins estimated by using the proposed method can be regarded as a reference in the design process for quantifying the sacrifice in stability margins to evaluate the tradeoff against improved time-domain tracking performance.

## References


[1] Seron, M. M., Braslavsky, J. H., and Goodwin, G. C., *Fundamental Limitations in Filtering and Control*, Springer-Verlag, London, United Kingdom, 1997, Chap. 3.

[2] Stein, G., "Respect the Unstable," *IEEE Control Systems Magazine*, Vol. 23, No. 4, 2003, pp. 12–25. doi:10.1109/MCS.2003.1213600.

[3] Zames, G., "Feedback and Optimal Sensitivity: Model Reference Transformations, Multiplicative Seminorms, and Approximate Inverses," *IEEE Transactions on Automatic Control*, Vol. 26, No. 2, 1981, pp. 301–320. doi:10.1109/TAC.1981.1102603.

[4] Zames, G., and Francis, B. A., "Feedback, Minimax Sensitivity, and Optimal Robustness," *IEEE Transactions on Automatic Control*, Vol. 28, No. 5, 1983, pp. 585–601. doi:10.1109/TAC.1983.1103275.

[5] Francis, B. A., and Zames, G., "On $\mathcal{H}_\infty$-Optimal Sensitivity Theory for SISO Feedback Systems," *IEEE Transactions on Automatic Control*, Vol. 29, No. 1, 1984, p. 16. doi:10.1109/TAC.1984.1103357.

[6] Kwakernaak, H., "Robust Control and $\mathcal{H}_\infty$-Optimization – Tutorial Paper," *Automatica*, Vol. 29, No. 2, 1993, pp. 255–273. doi:10.1016/0005-1098(93)90122-A.

[7] Nagamune, R., "Sensitivity Reduction for SISO Systems Using the Nevanlinna-Pick Interpolation with Degree Constraint," *14th International Symposium of Mathematical Theory of Networks and Systems*, Perpignan, France, 2000.

[8] Nagamune, R., "Closed-Loop Shaping Based on Nevanlinna-Pick Interpolation with a Degree Bound," *IEEE Transactions on Automatic Control*, Vol. 49, No. 2, 2004, pp. 300–305. doi:10.1109/TAC.2003.822853.

[9] Nagamune, R., and Blomqvist, A., "Sensitivity Shaping with Degree Constraint by Nonlinear Least-Squares Optimization," *Automatica*, Vol. 41, No. 7, 2005, pp. 1219–1227. doi:10.1016/j.automatica.2005.01.017.

[10] Apkarian, P., and Noll, D., "Nonsmooth $\mathcal{H}_\infty$ Synthesis," *IEEE Transactions on Automatic Control*, Vol. 51, No. 1, 2006, pp. 71–86. doi:10.1109/TAC.2005.860290.

[11] Apkarian, P., and Noll, D., "Nonsmooth Optimization for Multiband Frequency-Domain Control Design," *Automatica*, Vol. 43, No. 4, 2007, p. 724–731. doi:10.1016/j.automatica.2006.08.031.

[12] Apkarian, P., Dao, M. N., and Noll, D., "Parametric Robust Structured Control Design," *IEEE Transactions on Automatic Control*, Vol. 60, No. 7, 2015, pp. 1857–1869. doi:10.1109/TAC.2015.2396644.

[13] Apkarian, P., and Noll, D., "The $\mathcal{H}_\infty$ Control Problem is Solved," *AerospaceLab*, Vol. 13, No. AL13-01, 2017, pp. 1–11. doi:10.12762/2017.AL13-01.

[14] Apkarian, P., and Noll, D., "Optimization-Based Control Design Techniques and Tools," *Encyclopedia of Systems and Control*, Springer-Verlag, London, United Kingdom, 2020, pp. 487–494. doi:10.1007/978-1-4471-5102-9_144-2.

[15] Boyd, S., and Barratt, C., *Linear Controller Design: Limits of Performance*, Prentice-Hall, Upper Saddle River, NJ, 1991, Chap. 9.

[16] Skogestad, S., and Postlethwaite, I., *Multivariable Feedback Control Analysis and Design*, John Wiley & Sons, Chichester, United Kingdom, 2005, Chap. 2, p. 36.

[17] Kinnaert, M., "Right Half Plane Poles and Zeros and Robustness Limitations in Feedback Systems," *9th International Conference on Analysis and Optimization of Systems*, Antibes, France, 1990. doi:10.1007/BFb0120109.

[18] Lewin, D. R., "Robust Performance Specifications for Uncertain Stable SISO Systems," *International Journal of Control*, Vol. 53, No. 6, 1991, pp. 1263–1281. doi:10.1080/00207179108953674.

[19] Lewin, D. R., and Haim, D., "$H_\infty$-Mapping as a Tool for Defining Achievable Robust Closed-Loop Performance for SISO Systems," *Computers & Chemical Engineering*, Vol. 16, No. 8, 1992, pp. 793–803. doi:10.1016/0098-1354(92)80061-D.

[20] Christian, L., and Freudenberg, J., "Limits on Achievable Robustness Against Coprime Factor Uncertainty," *Automatica*, Vol. 30, No. 11, 1994, pp. 1693–1702. doi:10.1016/0005-1098(94)90072-8.

[21] Halpern, M. E., and Evans, R. J., "Robustness Result for Linear Continuous-Time SISO Systems," *13th IFAC World Congress*, San Francisco, CA, USA, 1996. doi:10.1016/S1474-6670(17)58140-9.

[22] Halpern, M. E., and Evans, R. J., "Maximally Robust Feedback Controller Design," *35th IEEE Conference on Decision and Control*, Kobe, Japan, 1996. doi:10.1109/CDC.1996.576942.

[23] Halpern, M. E., and Evans, R. J., "Maximal Stability Robustness Against Real Plant Coefficient Uncertainty," *European Conference on Control*, Brussels, Belgium, 1997. doi:10.23919/ECC.1997.7082236.

[24] Peters, A. A., and Salgado, M. E., "Performance Bounds in $\mathcal{H}_\infty$ Optimal Control for Stable SISO Plants With Arbitrary Relative Degree," *IEEE Transactions on Automatic Control*, Vol. 54, No. 8, 2009, pp. 1987–1990. doi:10.1109/TAC.2009.2023966.

[25] Mracek, C. P., *Tactical Missile Autopilots*, 2nd ed., Springer, Cham, Switzerland, 2021, pp. 2319–2325. doi:10.1007/978-3-030-44184-5_19.

[26] Ruth, M., Lebsock, K., and Dennehy, C., "What's New is What's Old: Use of Bode's Integral Theorem (circa 1945) to Provide Insight for 21st Century Spacecraft Attitude Control System Design Tuning," *AIAA Guidance, Navigation, and Control Conference*, Toronto, Ontario, Canada, 2010. doi:10.2514/6.2010-8428.

[27] Zhou, K., Doyle, J. C., and Glover, K., *Robust and Optimal Control*, Prentice Hall, Englewood Cliffs, NJ, USA, 1995, Chap. 9, pp. 230–231.

[28] Šebek, M., and Hurák, Z., "An Often Missed Detail: Formula Relating Peak Sensitivity with Gain Margin Less Than One," *17th International Conference on Process Control*, Štrbské Pleso, Slovakia, 2009.

[29] Chen, J., "Fundamental Limitation of Feedback Control," *Encyclopedia of Systems and Control*, Springer-Verlag, London, United Kingdom, 2020, pp. 487–494. doi:10.1007/978-1-4471-5102-9_156-2.

[30] Yuan, C., Liu, Y., Wu, F., and Duan, C., "Hybrid Switched Gain-Scheduling Control for Missile Autopilot Design," *Journal of Guidance, Control, and Dynamics*, Vol. 39, No. 10, 2016, pp. 2352–2363. doi:10.2514/1.G001791.

[31] Lee, C.-H., Jun, B.-E., and Lee, J.-I., "Connections Between Linear and Nonlinear Missile Autopilots via Three-Loop Topology," *Journal of Guidance, Control, and Dynamics*, Vol. 39, No. 6, 2016, pp. 1424–1430. doi:10.2514/1.G001565.

[32] Kim, J.-H., and Whang, I. H., "Augmented Three-Loop Autopilot Structure Based on Mixed-Sensitivity $H_\infty$ Optimization," *Journal of Guidance, Control, and Dynamics*, Vol. 41, No. 3, 2018, pp. 751–756. doi:10.2514/1.G003119.

[33] Lee, J., Cho, N., and Kim, Y., "Analysis of Missile Longitudinal Autopilot Based on the State-Dependent Riccati Equation Method," *Journal of Guidance, Control, and Dynamics*, Vol. 42, No. 10, 2019, pp. 2183–2196. doi:10.2514/1.G003679.

[34] Theodoulis, S., and Proff, M., "Robust Flight Control Tuning for Highly Agile Missiles," *Guidance, Navigation, and Control Conference, AIAA SciTech Forum*, Virtual, 2021. doi:10.2514/6.2021-1568.

2023-11-07

# Approximation of achievable robustness limit based on sensitivity inversion

Cho, Namhoon

AIAA

Cho N, Lee H-I. (2023) Approximation of achievable robustness limit based on sensitivity inversion. Journal of Guidance, Control, and Dynamics, Available online 7 November 2023
https://doi.org/10.2514/1.G007169